Low cycle fatigue life improvement of AISI 304 by initial and intermittent wire brush hammering

Kamel Makhlouf [a], Naziha Sidhom [a], Ammar Khlifi [a], Habib Sidhom [a,*], Chedly Braham [b]

[a] Laboratoire de Mécanique, Matériaux et Procédés (LR99ES05), ESSTT, University of Tunis, 5, Avenue Taha Husseïn, Montfleury, 1008 Tunis, Tunisia
[b] Laboratoire de Procédés et Ingénierie en Mécanique et Matériaux (PIMM-UMR CNRS 8006), ENSAM, 151, Boulevard de l'Hôpital, 75013 Paris, France

Keywords:
Stainless steel
Wire brush hammering
Residual stress
Fatigue crack
Fatigue life
Plasticity induced martensite

A B S T R A C T

The effects of hammering by wire brush as a method of improving low cycle fatigue life of highly ductile austenitic stainless steel AISI 304 have been investigated through an experimental study combining imposed strain fatigue tests and assessment of surface characteristic changes under cyclic loading by SEM examinations and XRD analysis. It has been shown that the fatigue life of wire brush hammered surface was increased by 307% at an imposed strain rate of 0.2% and only 17% at an imposed strain rate of 0.5%, comparatively to the turned surface. This increase in fatigue life is explained in terms of fatigue damage that is related to crack networks characteristics and stability which are generated during fatigue on both turned and wire brush hammered surfaces. The improvement of brushed surface is attributed to the role of the surface topography, the near surface stabilized compressive residual stresses and superficial cold work hardening on the fatigue crack network nucleation and growth. It is found that wire brush hammering produces a surface texture that favors, under cyclic loading, nucleation of randomly dispersed short cracks of the order of 40 μm in length stabilized by the compressive residual stress field that reached a value of $\sigma_0 = -749$ MPa. In contrast, turned surface showed much longer unstable cracks of the order of 200 μm in length nucleated in the machining groves with high tendency to propagate under the effect of tensile residual stress field that reached value of $\sigma_0 = 476$ MPa. This improvement is limited to strain rates lower than 0.5%. At higher strain rates, a cyclic plastic deformation induced martensitic phase alters furthermore the fatigue behavior by producing high cyclic strengthening of the bulk material. This phenomenon lead to a reduction in strain imposed fatigue life. It has also been established that wire brush hammering can be used as an onsite surface treatment to improve the residual fatigue life of components subjected to cyclic loading. The efficiency of this treatment is demonstrated if it is performed at a fraction of service lifetime N_i/N_r lower than 0.5.

1. Introduction

Austenitic stainless steels are very important commercial alloys used almost in all industries including automotive, domestic, nuclear, chemical and food processing because of their good mechanical properties combined with very good resistance to various forms of corrosion. These materials have also great aptitude for plastic deformation due to their high ductility. The most commonly used grade by weight, is AISI 304 stainless steel which, when used in aerospace, nuclear and chemical industries, revealed other risks of damage in service, including fatigue and corrosion fatigue that depend mainly on the surface topography and on the subsurface metallurgical and mechanical states. To improve the surface integrity, mechanical surface treatments such as laser shock peening [1,2], shot peening [3,4], burnishing [4,5], brushing [6,7] and deep rolling [2,8,9] have been performed on these surfaces. These treatments proved to produce significant improvements in terms of endurance limit [3,6,7] and fatigue crack propagation resistance [1] as well as stress corrosion resistance [10]. These improvements were largely attributed to changes in the surface topography and hardness, compressive residual stress state and in some cases to phase changes such as a transformation induced plasticity (TRIP).

Laser peening applied on SUS304 and SUS316L austenitic stainless steels converted the initial residual stress state near the surface from tensile to compressive one that reached values up to −1100 MPa for SUS304 and −780 MPa for SUS316L respectively. This compressive residual stress reached depths as high as 1 mm. As a result, the treatment prevented the initiation of SCC and the propagation of existing pre-cracks in an environment where cracks were supposed to accelerate. The fatigue strength was increased by a factor of 40–70% for the SUS 316 [1]. Fathallah et al. [3] reported a beneficial effect of shot peening on high cycle fatigue of SAE 3415

* Corresponding author. Tel.: +216 71 496066; fax: +216 71391166.
E-mail addresses: habib.sidhom@gmail.com, habib.sidhom@esstt.rnu.tn (H. Sidhom).

caused by compressive residual stress and surface work hardening generated by shot peening in spite of the formation of superficial defects and surface imperfections. This improvement is reported for only a standard 100% coverage whereas for a severe condition of 1000% coverage, the treatment became detrimental due to formation of excessive superficial defects and micro-geometrical imperfections. Nikitin et al. [2] reported that residual stress stability generated by laser shock peening and deep rolling of AISI 304 stainless steel are found to enhance significantly the isothermal stress controlled fatigue behavior only at low temperatures but at temperatures above 400 °C, stress relaxation reduces this enhancement. Sidhom et al. [7] investigated the effects of wire brushing on the fatigue resistance of machined surfaces and reported that brushing produced compressive residual stresses in the same order as the ones generated by shot peening with the advantage of producing high surface quality to enhance the fatigue behavior by a factor of 20–30% for the aluminum alloy AA5083H11. Ben Fredj et al. [6] investigated the effects of wire brushing on the ground surfaces of AISI 304. He applied 3 point bending elastic strain controlled fatigue of notched ground samples and found that the brushing operation leads to a higher micro-geometrical quality of the surface that increased the endurance limit at 2×10^6 cycles by 26%. This process raised the fatigue strength from 226 MPa to 285 MPa. It appears that this improvement in fatigue decreases rapidly when lower cycles or higher strain fatigue is considered. Moreover, in this high cycle fatigue regime, Ben Fredj did not observe a phase transformation induced by fatigue deformation as observed in other cases [11,12]. Mei and Morris [13] found that the deformation induced martensitic transformation has significant effects on fatigue crack propagation in 304 stainless steel in the near threshold and in the Paris regime but these effects decrease as load ratio or mean stress increases. He added that this decrease in growth rates is the result of the perturbation of the stress field at the tip of the propagating crack and that the crack deflection and the brittleness of the freshly induced martensitic phase could contribute, as well, to this behavior. Topic et al. [14] reported that an amount of deformation induced martensite lower than 20% acts beneficially on fatigue behavior of low strength AISI 304 stainless steel by retarding the crack initiation and lowering the growth rates hence raising the fatigue limits and producing ductile fatigue striations whereas amounts greater than 20% degrade the fatigue behavior of the steel by promoting more rapid crack initiation and producing brittle fracture.

The shot peening treatment remains the most widely used despite its disastrous effects on the micro-geometric quality of the surface arising from the impact of hard particles on the ductile material. Such damages have proven to reduce resistance to localized corrosion which is one of the main selection criteria of these materials. In this work, a less aggressive technique which is more economical and easier to implement was chosen. The hammering by wire brush can replace the shot peening with profitability and efficiency that were demonstrated when applied on ground 304 stainless steel surfaces in the high cycle, elastic strains controlled fatigue using 3 point bending [6]. In addition, wire brush hammering can be used as a process to improve the surface lifetime of components subjected to cyclic loading as well as an intermittent process to extend the remaining surface lifetime of components subjected to plastic strain controlled fatigue.

The present work aims at proving the numerous technical and economical advantages of the wire brush hammering as an industrial surface mechanical treatment of ductile material parts. Among these advantages, an easy way to implement on line production, low cost comparatively to other surface treatment processes and the technical possibility to generate a substantial compressive residual stress without surface damage. The role of surface topography, stabilized surface compressive residual stress and cyclic plastic induced martensite on the fatigue crack nucleation and growth has been studied by X-ray diffraction and SEM examination. The beneficial effect of wire brush hammering of AISI 304 on fatigue life has been assessed as an initial and an intermittent treatment by strain controlled fatigue tests. The dependence of this technique on the imposed strain rate has also been investigated to establish the limiting parameters for the improvement.

2. Material and experimental procedures

2.1. Material

The material investigated in this study is an AISI 304 grade austenitic stainless steel. The microstructure of the material is shown in Fig. 1. The chemical composition and the tensile mechanical properties in the solution treated condition of the studied steel are given in Tables 1 and 2 respectively.

2.2. Wire brush hammering

Wire brush hammering was applied to the fatigue samples of the unstable AISI 304 (Fig. 2), previously machined by turning. The cutting parameters for the machining process are given in Table 3. The wire brush hammering operations were conducted on the turned surfaces using stainless steel wire brush under conditions given in Table 4. The brush used in this study is illustrated in Fig. 3 and its characteristics are given in Table 4.

2.3. Performed tests

2.3.1. Surface characterization tests

Micro-structural characterization of machined and wire brush hammered surfaces was carried out by metallographic examination followed by X-ray diffraction phase analysis. Surface hardening induced by deformation or by phase transformation was evaluated by micro-hardness ($Hv_{0.05}$) measurements according to ASTM: E384-11e1. Near surface residual stresses were determined by X-ray diffraction using the operating conditions given in Table 5 and in accordance with NF EN 15305-2009 standard [15].

2.3.2. Fatigue tests

Tension–compression low cycle fatigue tests ($R_\sigma = -1$) were performed at different imposed total strain rates of $\Delta\varepsilon_t/2 = 0.1\%$, 0.2%, 0.3%, 0.5%, 0.7% and 1% on an MTS closed loop servohydraulic test machine. The test samples were prepared according to ASTM:

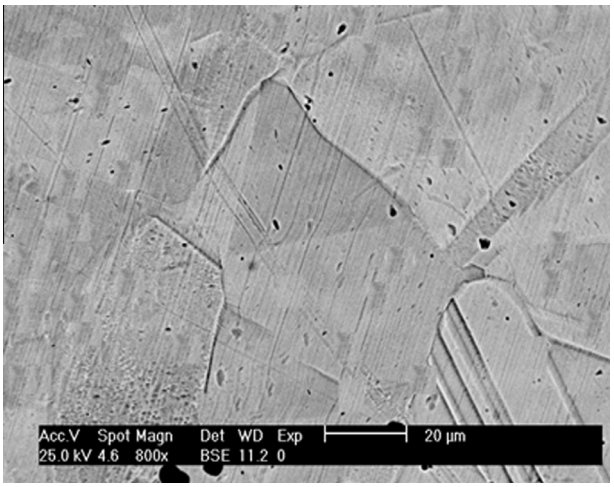

Fig. 1. Structure of the AISI 304 stainless steel in the solution treated condition.

Table 1
Chemical composition of AISI 304 stainless steel (weight%).

Grade	Chemical composition (weight%)								
	C	Si	Mn	N	Cu	Cr	Ni	Mo	Fe
AISI 304	0.05	0.41	1.14	0.04	0.34	18.04	9	0.19	Balance

E606-12. The frequency was set at 0.1 Hz. The fatigue tests were conducted until fracture of the sample occurred. Hysteresis loops were recorded during the fatigue tests to assess the impact and the improvement limitation of the wire brush hammering operation on the total fatigue life of the sample. In addition, intermittent brushing operations were carried out on samples during the fatigue loading to assess the improvement of their residual life.

2.3.3. Fatigue crack examination

Histograms of crack length and depth distributions have been established for quantitative analysis of the role of surface characteristics on the initiation and propagation of fatigue crack resistance. The phenomenon of cyclic relaxation of residual stresses on the surface sample was followed for two total imposed strain rates of $\Delta\varepsilon_t/2 = 0.3\%$ and $\Delta\varepsilon_t/2 = 1\%$. Verification of the martensitic phase transformation induced by the cyclic plastic deformation which was accumulated during fatigue loading at different imposed strain rates was performed by X-ray diffraction of the fracture surfaces.

The role of wire brush hammering on the initiation and propagation of fatigue cracks was determined by scanning electron microscopy. In addition, the evolution of surface crack networks was investigated. The damage mode was determined by microscopic examination of a sample that had been tested at a total strain $\Delta\varepsilon_t/2 = 0.7\%$ and polished.

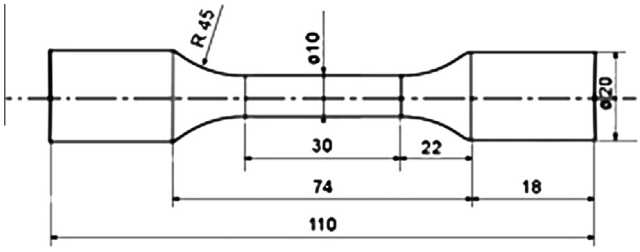

Fig. 2. Fatigue test sample.

Table 3
Turning conditions.

Cutting speed, V_c (m/mn)	Feed rate (mm/rv)	Depth of cut (mm)	Carbide tool beak radius (mm)	Environment
51	0.05	0.4	0.4	Soluble oil (20%)

Table 4
Wire brush hammering conditions.

Brush characteristics		Brushing conditions	
Brush diameter	$D = 230$ mm	Brush rotation speed	$V_s = 2000$ rpm
Wire diameter	$\varnothing = 0.1$ mm	Table's feed speed	$V_f = 50$ mm/min
Wire length	$L = 80$ mm	Number of passes	$N = 10$
Wire material	Stainless steel	Compression percentage[a]	3%

[a] Used length/wire length.

3. Results

3.1. Surface quality evaluation

The quality of the prepared surfaces is evaluated via the surface roughness measurements, the surface defects distribution, the microstructural changes and the residual stress levels in the process affected layers. Table 6 summarizes the values of the surface characteristics parameters for surfaces obtained by turning, and by wire brush hammering of the fatigue samples.

3.1.1. Micro-geometric quality

The surface roughness determined by SEM examination has shown grooves obtained by the machining process, as revealed in Fig. 4, whereas brushing appears to illuminate these machining grooves and produce surface overlaps as a result of the successive strikes of the steel wires of the brush, leading to a micro-topography of the surface which is similar to a blasted surface. These features are seen in Fig. 5.

Superimposition of the two roughness profiles, as shown in Fig. 6, reveals a material transport phenomenon accompanying the brushing operations. In terms of roughness, wire brush hammering slightly changes the values of R_a from 2.5 μm in the machined condition to 3.8 μm in the brushed condition. In addition, brushing seems to have the advantage of clearing the surface from the previously seen machining grooves.

3.1.2. Microstructural change

Work hardening induced by both surface machining and brushing was investigated by micro-hardness ($Hv_{0.05}$) measurements and by X-ray diffraction. Micro-hardness profiles superimposition shows a stronger hardening gradient for the wire brush hammered surface compared to the machined one as seen in Fig. 7. A surface hardness of 510 Hv is measured for the wire brush hammered material whereas only a value of 375 Hv is measured for the machined surface. Therefore, the rate of the hardening of the surface with respect to the bulk material is increased by 163% and 108% for the wire brush hammered and for the turned surfaces respectively as shown in column B of Table 6. The extent of the cold work hardening is comparable for both surface preparation modes (turned and brushed) and it reached 200 μm underneath the surface (Fig. 7).

X-ray diffraction using cobalt Kα rays (1.79 Å) has been used to assess the phase changes that could occur during the wire brush

Table 2
Mechanical properties of AISI 304 stainless steel.

Material	Tensile mechanical properties					Balk hardness (Hv)
	Yield strength R_e (MPa)	0.2% Offset yield strength $R_{p0.2}$ (MPa)	Tensile strength R_m (MPa)	Young's modulus E (GPa)	Elongation A_r (%)	
AISI 304	260	320	615	193	58	171

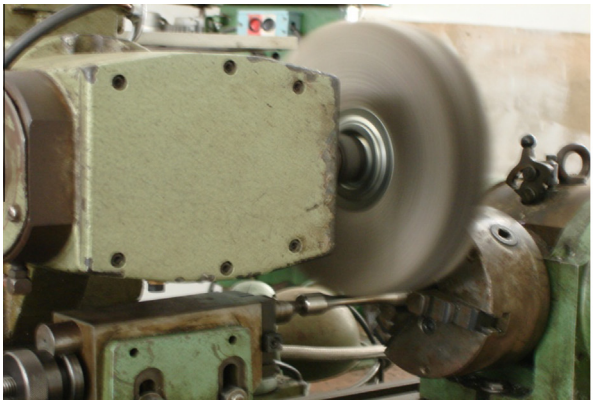

Fig. 3. Wire brush hammering apparatus.

Table 5
X-rays diffraction conditions.

Radiation	λ Mn Kα × λ = 0.2102 nm
Voltage	20 kV
Current	5 mA
X-ray diffraction planes	{3 1 1} $2\theta \approx 152°$
Beam diameter	2 mm
$\varnothing$ Angles	0° and 90°
Ψ Oscillation	±3°
Ψ Angles	−37.27–33.21–28.88 −24.09–18.43 −10.52 0.00 14.96 21.42 26.57 31.09 35.26 39.23

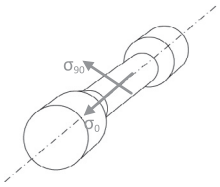

hammering operation of the AISI 304 stainless steel. Data analysis of samples does not reveal the presence of any specific ferritic phase such as martensite $\acute{\alpha}$ or ε (Fig. 8). Such phases are expected to be induced by plastic deformation and to be probably dependent on the strain rate and temperature. However, the presence of only austenite peaks in the X-ray diffractogram indicates that the generated heat in turning and wire brush hammering of the metastable AISI 304 prevents the martensite formation despite the high processes induced plastic rates in the near surface.

3.1.3. Residual stress state

Machining and wire brush hammering operations induce residual stresses in the processing affected layers. The near surface residual stress levels are reported in column C of Table 6. It shows that due to turning, tensile residual stresses of $\sigma_0 = 339$ MPa in the cutting direction and $\sigma_{90} = 476$ MPa in the feed direction are produced on the surface of the sample, whereas the mechanical brushing induces, under the conditions defined in this study, as expected, compressive residual stresses that reach values of $\sigma_0 = -622$ MPa and $\sigma_{90} = -750$ MPa in the same directions respectively.

3.2. Fatigue life evaluation

Fatigue lifetime results of the initial and intermittent wire brush hammering are compared to those of the turned state in order to evaluate the rate of improvement resulting from these treatment conditions.

3.2.1. Effect of initial wire brush hammering

Analysis of the fatigue results, based on lifetime for each imposed strain rate, shows a considerable gain in the number of cycles to failure produced by the brushing treatment. This gain is limited to total strain rates $\Delta\varepsilon_t/2 \leqslant 0.5\%$, corresponding to loading amplitudes of $\Delta\sigma/2 < 248$ MPa, as shown in Table 7. The fatigue lifetime is, at least, four times higher when the imposed strain rate $\Delta\varepsilon_t/2 \leqslant 0.2\%$ of the total strain (or $\Delta\varepsilon_p/2 \leqslant 0.132\%$ of the plastic deformation). This represents 307% of fatigue life rate improvement. When the imposed strain amplitude becomes more important, e.g. greater than 0.5%, the beneficial effect of the mechanical brush hammering after machining is completely annihilated or even reversed, as shown in Table 7 where lifetimes generated at $\Delta\varepsilon_t/2 = 0.7\%$ or 1%, are slightly lower for the brushed samples than for just the turned ones. Consequently, 0.5% total imposed strain rate could be considered as limiting parameter for improvement fatigue life by wire brush hammering surface treatment.

3.2.2. Effect of intermittent wire brushing

Limitation of intermittent wire brushing; as an onsite improvement method of components residual service life; has been determined. The optimum fraction of lifetime to perform the brushing operation is also identified. In this case, intermittent brushing treatments at various lifetime fractions $N_i/N_r = 0.16$, 0.25 and 0.5 on the turned surface during cyclic loading at deformation rates of 0.2%, 0.3% and 0.5% have been performed in order to evaluate experimentally the residual fatigue life improvement. The results, summarized in Table 8, show that intermittent brushing is an efficient process to extend the residual service lifetime of AISI 304 components loaded at imposed strain rates $\Delta\varepsilon_t/2 \leqslant 0.5\%$. This treatment is more beneficial when it is performed at low N_i/N_r values. In all cases, brushing performed at N_i/N_r higher than 0.5 is considered as inefficient improvement operation. Nevertheless, significant improvement in the residual lifetime for $\Delta\varepsilon_t/2 = 0.2$, ranging from 216% to 16% is reported when brushing operation is applied on the surface sample at 16% and 50% of the total life of the component respectively. For the strain rates of $\Delta\varepsilon_t/2$ of 0.3 and 0.5, the improvements of the residual life are less significant. They range between 45% and 11%.

3.3. Role of cyclic induced surface characteristics changes

The fatigue life improvements reported for the initial and intermittent wire brushing are likely due to the cyclic induced surface

Table 6
Characteristics for turned and brush hammered surfaces of AISI 304.

Finishing mode	A Roughness (μm)		B Microhardness ($Hv_{0.05}$)			C Near surface residual stress level (MPa)		D Surface texture
	R_a	R_t	Near surface $(Hv)_s$	Bulk material $(Hv)_c$	Strain hardened thickness (μm)	σ_0	σ_{90}	
Turning	2.51	10.04	375	180	190	$339^{\pm 20}$	$476^{\pm 20}$	Machining grooves
Turning + brushing	3.83	15.32	510	180	200	$-622^{\pm 35}$	$-750^{\pm 15}$	Overlaps

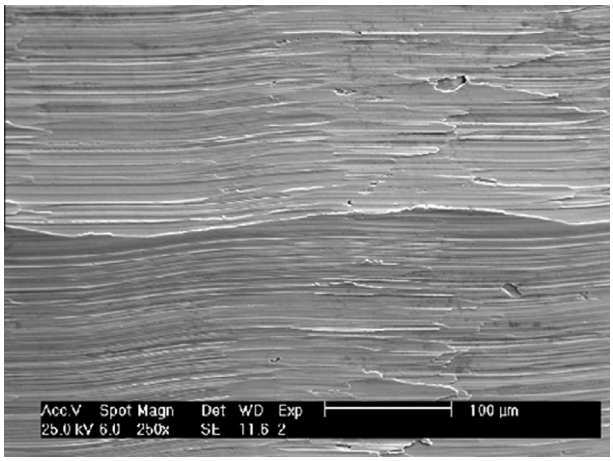

Fig. 4. Surface texture of turned AISI 304 stainless steel.

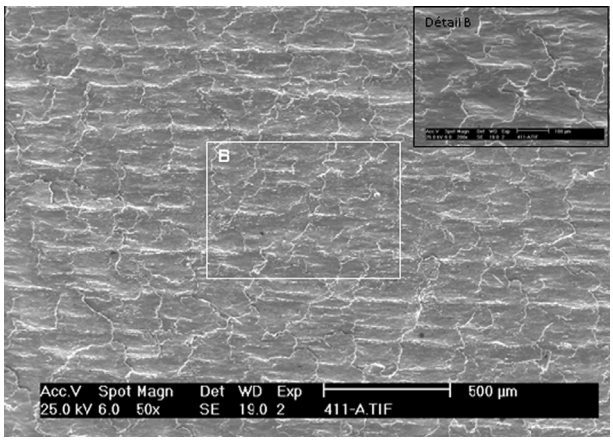

Fig. 5. Surface texture of wire brush hammered AISI 304 stainless steel.

characteristics changes and their effects on fatigue cracks nucleation and growth.

3.3.1. Effect of stabilized residual stress

The beneficial effects of compressive residual stresses induced by initial brushing operation could be reduced or annihilated by cyclic relaxation as the imposed strain rate is increased. Indeed, experimental X-ray diffraction measurements, reported in Table 8, show an important relaxation of the near surface residual stress. This relaxation is more significant in the cyclic loading direction than in the transverse one. Moreover, this phenomenon is observed for both surface mode preparation turned and brushed. That is why fatigue life improvement resulting from brushing operation decreases as the compressive residual stresses relaxes furthermore for imposed strain rates $\Delta\varepsilon_t/2 \leqslant 0.7\%$ ($\Delta\varepsilon_p/2 \leqslant 0.52\%$). For a strain rate $\Delta\varepsilon_t/2 = 1\%$, a different phenomenon seems to be operating since compressive residual stresses are increased again.

3.3.2. Effect of plastic deformation induced martensite

Cyclic consolidation curves of wire brushed surfaces show a strengthening followed by a softening phase before fracture for imposed strain rates lower than 1% (Fig. 9). It is important to notice that cyclic strengthening is more important as the strain rate is higher. Nevertheless, for the strain rate of 1%, a second high strengthening is observed just before fracture (Fig. 9). X-ray diffraction analysis, at that level, reveals transformation induced plasticity (TRIP) martensite $\acute{\alpha}$ phase as shown in Fig. 10. This transformation did not occur for the lower strain rates (0.7%, 0.5% and 0.3%). This TRIP is likely responsible for the increase of compressive residual stress levels in the main loading direction. Whereas, residual stress relaxation, is observed for strain rates lower than 1% as shown in Table 8. The association of the plastic deformation induced martensite–slip bands is also observed by SEM examination of wire brushed and loaded at a strain rate of 1% of surface fatigue sample (Fig. 11).

3.3.3. Effect of surface texture

3.3.3.1. Basic mechanisms. The damage mode in low cycle fatigue was evaluated by SEM metallographic examination of the samples surfaces loaded at $\Delta\varepsilon_t/2 = 0.7\%$ at different periods marked (a, b, c and d) on the consolidation curve ($\Delta\sigma/2$ versus N) given in Fig. 12. These samples were polished and etched before the fatigue tests. Metallographic examination of these surfaces revealed the following:

- After only 10 loading cycles, the material strengthens slightly resulting in an increase of $\Delta\sigma/2$ from 377 MPa to 405 MPa. This strengthening is caused by cyclic plasticity through the appearance of low density slip lines with few steps as shown in Fig. 12a. This phenomenon is referred to as stage I.
- After 100 loading cycles, the material undergoes softening as $\Delta\sigma/2$ goes down from 405 MPa to 358 MPa. This is referred to as stage II.

$$\Delta\sigma/2 = 377\ \text{MPa} \overset{\text{Stade I}}{\rightarrow} \Delta\sigma/2 = 405\ \text{MPa} \overset{\text{Stade II}}{\rightarrow} \Delta\sigma/2 = 358\ \text{MPa}$$

At this level, the deformation is localized in the persistent slip bands that become denser producing more steps as shown in Fig. 12b.

- After 1000 cycles, the stress amplitude decreases furthermore to 340 MPa and few micro-cracks appear along the slip lines as shown in Fig. 12c. These are stage III features.

$$\Delta\sigma/2 = 377\ \text{MPa} \overset{\text{Stade I}}{\rightarrow} \Delta\sigma/2 = 405\ \text{MPa} \overset{\text{Stade II}}{\rightarrow} \Delta\sigma/2 = 358\ \text{MPa} \overset{\text{Stade III}}{\rightarrow} \Delta\sigma/2 = 340\ \text{MPa}$$

At this level, micrographic analysis reveals widespread damage characterized by the appearance of micro-cracks at the grain scale associated with very dense persistent slip bands. It should be noted that these micro-cracks are substantially perpendicular to the axis of the applied load (Fig. 12c).

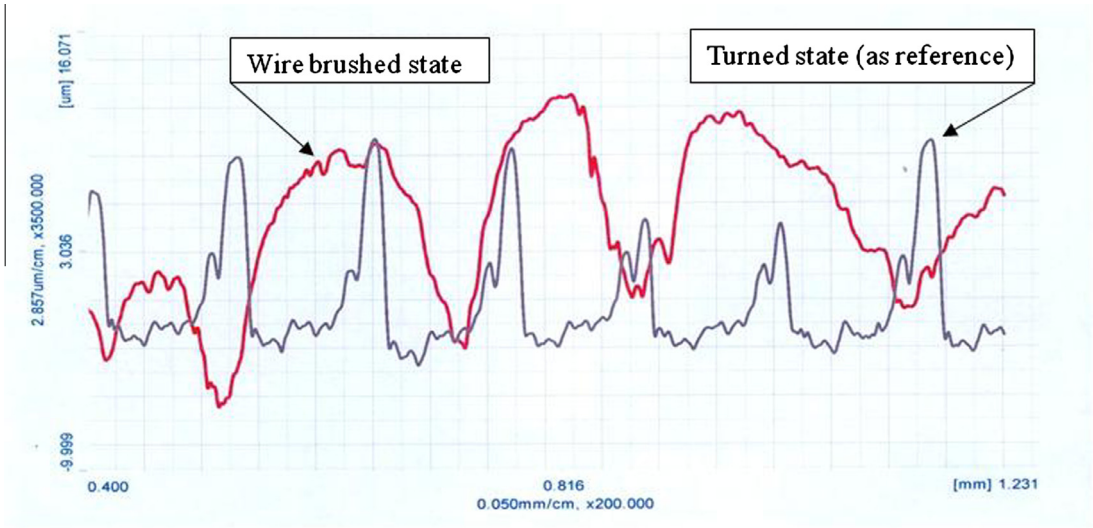

Fig. 6. Superimposition of machined and wire brush hammered surface roughness profiles of AISI 304 stainless steel.

Additional loading leads to further accumulation of damage to form networks of interconnected micro-cracks as shown in Fig. 12d. These micro-crack networks will grow to produce the final fracture of the sample.

It is important to notice that for the smooth surface (electro polished), the fatigue crack nucleation and growth are controlled by the deformation microstructure such as the number and the direction of persistent slip bands and the inter-bands spacing. This phenomenon produces crystallographic aspect of surface fatigue crack networks (Fig. 12). An analysis of this phenomenon for the strain rate $\Delta\varepsilon_t/2 = 0.3\%$ is discussed in the next two paragraphs.

3.3.3.2. Role of turned surface texture. For the turned surface loaded at a strain rate of $\Delta\varepsilon_t/2 = 0.3\%$ until fracture, long cracks of about 200 μm in length were observed on the surface near the main fracture, as seen in Fig. 13. These cracks are obviously located in the machining grooves that constitute preferential sites for crack initiation as they are micro-stress concentration sites. These micro-cracks are likely to initiate at the persistent slip bands created on the surface layer which is under the machining induced tensile residual stress field (+476 MPa). These micro-cracks grow quickly and coalesce to produce premature failure (N_r = 64,650 cycles).

3.3.3.3. Role of brushed surface texture. For the brushed surface loaded at a strain rate of $\Delta\varepsilon_t/2 = 0.3\%$ until fracture, much shorter micro-cracks, of the order of 50 μm in length are observed randomly on the surface as seen in Fig. 14. These cracks which are small initiate in the topographical features generated by the hammering of the surface by the steel wires of the brush. These cracks which are stable with respect to propagation by the effects of the brushing induced compressive residual stress field (−622 MPa). This stress field impedes considerably their growth and coalescence even after partial cyclic relaxation. These observation explain the fatigue life improvement produced by the brushing operation (112,900 cycles) comparatively to the turned surface (64,650 cycles) loaded under the same conditions ($\Delta\varepsilon_t/2 = 0.3\%$).

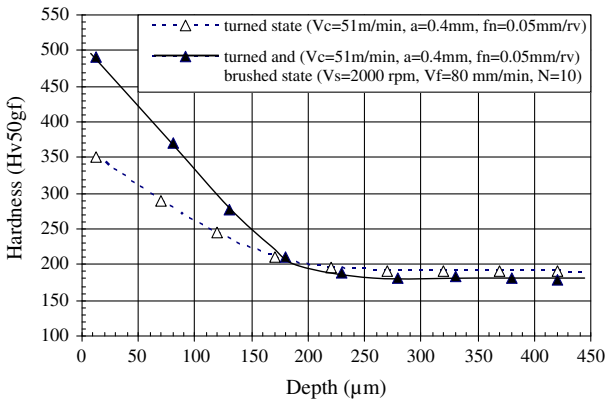

Fig. 7. Micro-hardness profiles in the subsurface layers of the turned and wire brush hammered AISI 304 steel surfaces.

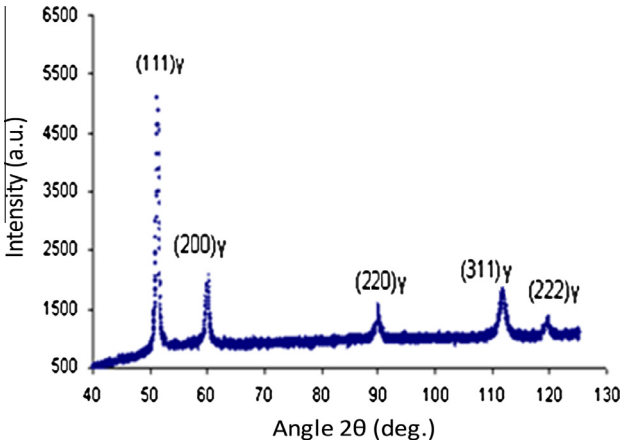

Fig. 8. Phase analysis of the wire brush hammered surface of the AISI 304 steel.

4. Discussion

It was established in this paper the beneficial effects of hammering by wire brush as a method to improve low cycle fatigue resistance of AISI 304 austenitic stainless steel through an experimental study combined with macroscopic and microscopic fatigue damage evaluation. This improvement seems to be comparable to other surface treatment processes like shoot peening, sand blasting and hammering. The limitation of the improvement produced by wire brush hammering was determined as an initial and an intermittent surface treatment. This limitation is dependent on the imposed strain rates. The fatigue life improvement of the brushed

Table 7
Life time improvement by mechanical brushing.

Material	Low cycle fatigue test conditions				Number of cycles to fracture N_r		
	Test temperature Θ (°C)	Frequency (Hz)	Load ratio	$\frac{\Delta\varepsilon_t}{2}$ (%)	Surface finishing mode		Improvement rate[a] (%)
					Turning	Turning + brushing	
AISI 304	$T = 20$	$f = 0.1$	$R = -1$	0.1	Not fractured	Not fractured	–
				0.2	188,509	768,362	307
				0.3	64,650	112,900	74
				0.5	7650	9015	17
				0.7	2740	2564	Detrimental effect
				1	1152	894	Detrimental effect

[a] Improvement rate with respect to turning surface.

Table 8
Assessment of the effects of intermittent brushing on the remaining life of components manufactured from AISI 304.

Imposed deformation rate $\frac{\Delta\varepsilon_t}{2}$ (%)	Lifetime of component after turning N_r (cycle)	Fraction of lifetime in service N_i/N_r	Total lifetime of brushed component N_r (cycle)	Improvement rate of residual lifetime, $\Delta N_{residual}$ (%)
0.2	188,509	0	768,362	307
		0.16	596,411	216
		0.25	289,467	53
		0.5	218,804	16
0.3	64,650	0	112,900	75
		0.16	87,950	45
		0.25	79,435	30
		0.5	68,436	11
0.5	7650	0	9915	35
		0.16	9550	30
		0.25	9127	24
		0.5	8650	15

AISI304 has been discussed on the basis of the influencing factors such as surface topography, surface hardening, residual stress state, and microstructural changes. All these parameters control directly or indirectly the initiation and the propagation stages of fatigue cracks.

4.1. Fatigue life improvement resulting from the initial hammering

Wire brush hammering which acts on the surface of the sample modifies significantly the surface characteristics like texture, hardness, near-surface residual stress state and plastic induced phase transformation. The resulting fatigue improvement is the consequence of the balanced contribution of these modifications.

4.1.1. Contribution of surface texture

In contrast to shot peening, hammering by wire brushing of the ductile AISI 304 stainless steel does not alter significantly the surface roughness and does not induce large defects [6]. It is found that the arithmetic average surface roughness, R_a, increased slightly from 2.5 to 3.8 μm as a result of wire brush hammering whereas the maximum surfaces roughness, R_t, increased significantly from 10.0 to 15.3 μm. These results are different from those generated by Ben Fredj et al. [6] on ground surfaces of AISI 304 stainless steel where he reported a decrease in R_t values by 60% and no change in R_a when the surface has received a brush hammering treatment. In addition, like shot peening, wire brush hammering treatment seems to reduce or eliminate the surface grooves produced during machining operation which was an anterior generated surface process. Obviously, these surface grooves represent preferential sites for micro-stress concentration. Therefore, wire brush hammering modifies the surface texture which is marked by a specific topography such as overlaps as a result of the impact of the brush wires on the surface. These features, with much less depth than that of the grooves, regularly cover the surface of the sample. This phenomenon led to the formation of short fatigue crack networks that retard the crack coalescence and propagation under cyclic loading. This explains partially, the improvement produced by the brushing treatment comparatively to the turned surface that is characterized by long cracks localized in the machining grooves as seen in Figs. 13 and 14 respectively.

4.1.2. Contribution of surface strain work hardening

The machining process induces cold work hardening (300 Hv) on the surface comparatively to the bulk material (200 Hv) whereas subsequent wire brush hammering produced much harder surface that reached a value of 510 Hv. This hardness decreased with depth to reach the value of the bulk material hardness at around 200 μm from the surface. This high surface hardness contributes to the enhancement of fatigue crack initiation resistance at the near surface. These results are in good agreement with those generated by Ben Fredj in which he reported a 26% increase in the polycyclic fatigue life and an increase of the endurance limit from 226 MPa to 285 MPa of a brushed but ground AISI 304 stainless steel surfaces [6]. The same improvement rate was reported by Sidhom for shot peened and for brushed aluminum alloys [16,17].

4.1.3. Contribution of residual stress

It is well known that the residual stress has a determinant effect on the nucleation and growth of fatigue cracks during cyclic loading. The tensile residual stress exhibits a detrimental effect by promoting crack initiation and propagation whereas the compressive residual stress tends to delay the nucleation phase and to slow the propagation phase [3,18].

Indeed, turning process produced tensile residual stress in both directions ($\sigma_0 = 339$ MPa in the loading direction and $\sigma_{90} = 476$ MPa in the transverse direction) and subsequent wire

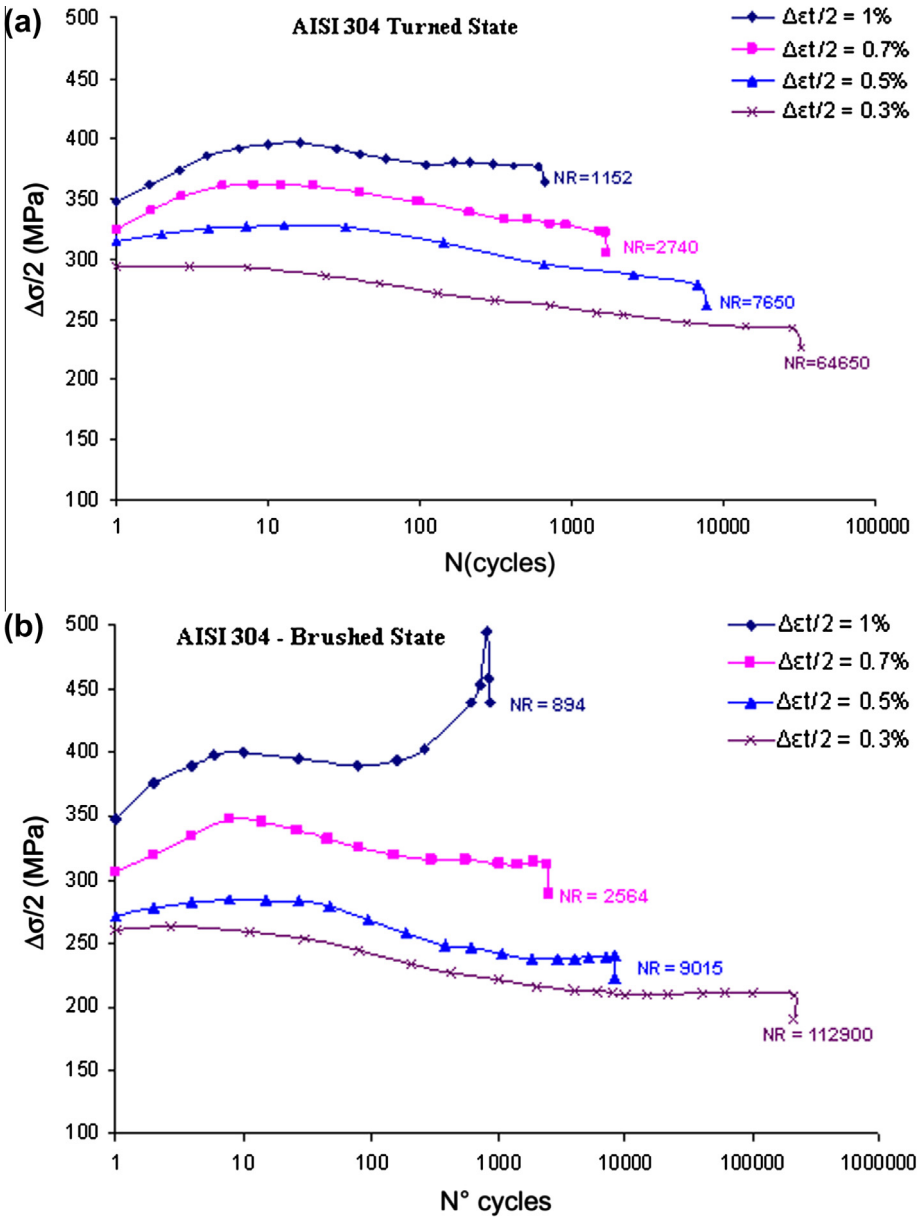

Fig. 9. Effects of turning (a) and wire brush hammering and (b) on the cyclic response of AISI 304 stainless steel at different strain rates.

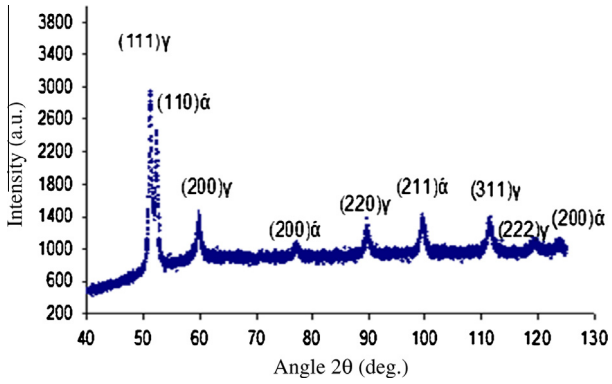

Fig. 10. Wire brush hammering of AISI 304 showing austenite γ and martensite ά after cyclic plastic deformation at ($\Delta\varepsilon_t/2 = \pm 1\%$).

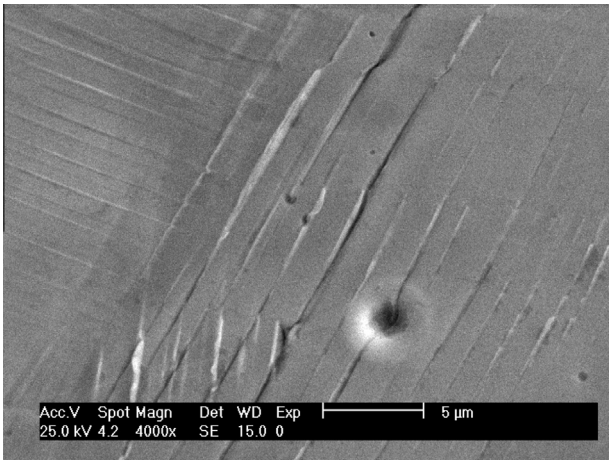

Fig. 11. Transformation induced martensite–slip bands interaction of wire brush hammered sample during fatigue at a strain rate $\Delta\varepsilon_t/2 = \pm 1\%$.

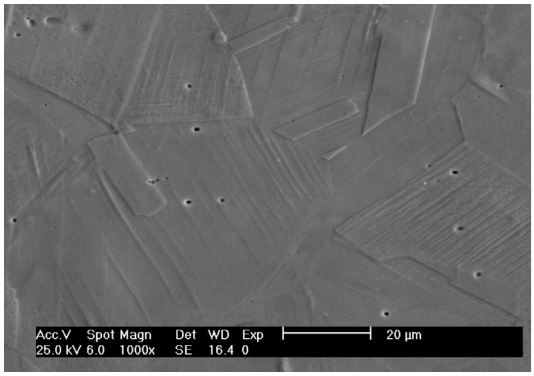

(a) Localized deformation in persistent slip bands produced after 10 cycles.

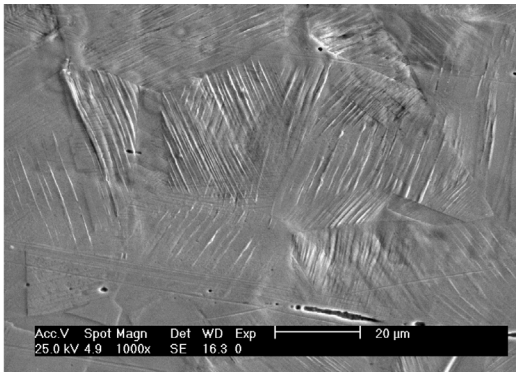

(b) Denser persistent slip bands observed after 100 cycles.

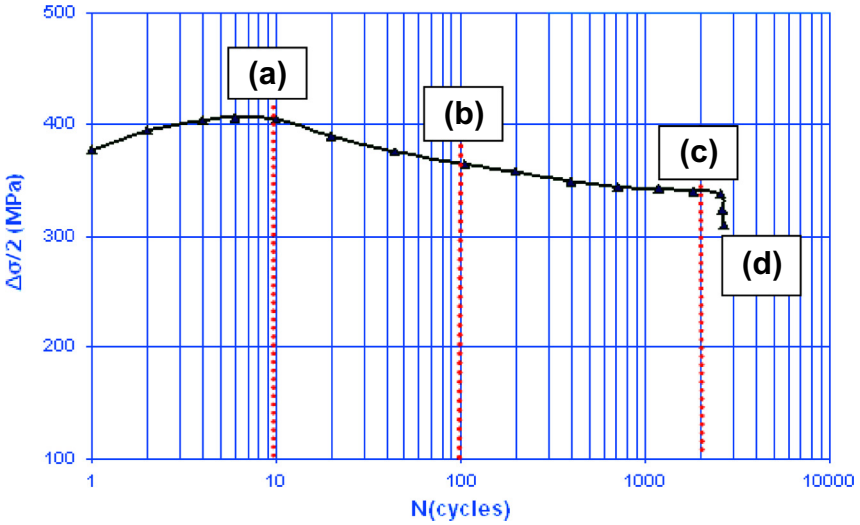

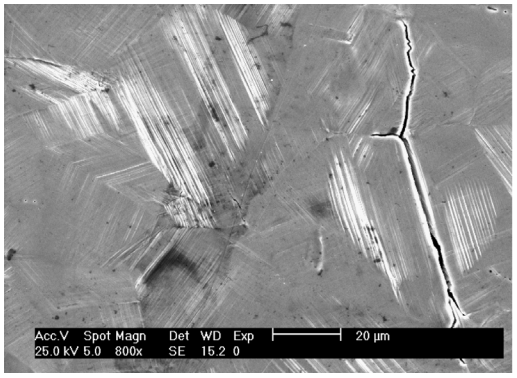

(c) Appearance of micro-cracks at the grain scale after 1000 cycles.

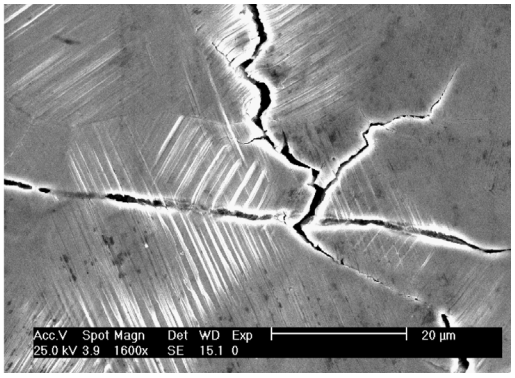

(d) Coalescence of these micro-cracks to produce the final fracture.

Fig. 12. Damage mode in low cycle fatigue in AISI 304 stainless steel.

brush hammering induced compressive residual stress field ($\sigma_0 = -622$ MPa and $\sigma_{90} = -750$ MPa in the same directions respectively). These residual stress distributions relax significantly, under imposed cyclic strain loading lower than 0.7% for both turned and brushed surfaces as seen in Table 9. This relaxation phenomenon occurs basically during the first 100 loading cycles to attain a stabilized state that controls the nucleation and growth of fatigue cracks for both surface preparation modes.

It is clear that the brushed surface has an advantageous texture in which fatigue crack nucleation network are more stabilized by the compressive residual stress field leading to a higher fatigue life comparatively to the machined surface. For the turned surface, unstable long cracks coalesce and propagate rapidly in a tensile residual stress field or low plastic cyclic induced compressive residual stress field. As the strain rate is increased, the beneficial effects of the brushing operation are reduced as a result of cyclic stress relaxation as shown in Table 9. These results are in good agreement with those obtained for shot peened surfaces of ductile material [16,17,19] and brushed surface of Aluminum alloys [7,20]. Sano et al. investigated the effects of laser peening without protec-

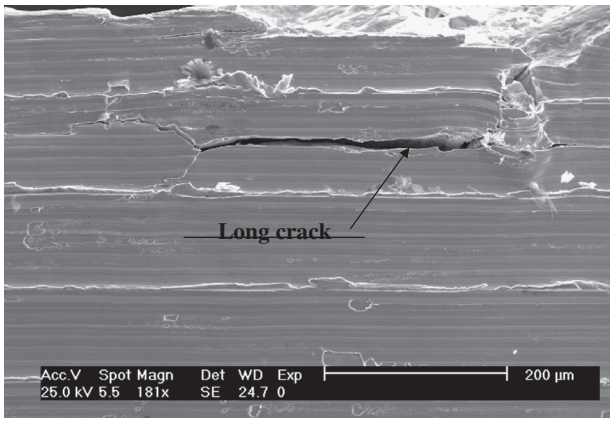

Fig. 13. Crack initiation sites of the turned sample. Micrograph taken at 30 µm from the main fracture surface ($\frac{\Delta\varepsilon_t}{2}$ = 0.3%, N = 64,650 cycles).

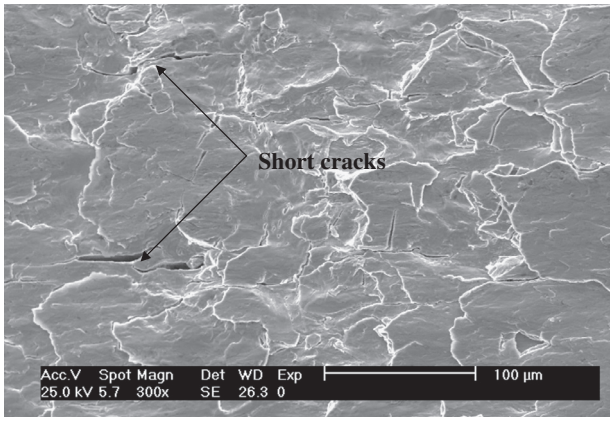

Fig. 14. Crack initiation sites of the turned and wire brush hammered sample. Micrograph taken at 30 µm from the main fracture surface ($\frac{\Delta\varepsilon_t}{2}$ = 0.3%; N = 112,900 cycles).

tive coating on crack initiation and found that the conversion of a tensile residual stress to a compressive one improved significantly the crack initiation stage and even inhibited the pre-existing small cracks from propagating [1].

4.1.4. Contribution of induced martensite

The XRD phase identification reveals the formation of a martensitic phase $\acute{\alpha}$ induced by brushing and cyclic plastic deformation as shown in Fig. 10 obtained only for a plastic strain of $\Delta\varepsilon_t/2$ = 1%. For the same rate, the turned surface did not exhibit plastic induced martensite. For strain rates lower than 1%, no martensite has been detected; neither for the turned nor for brushed samples. This indicates that the martensite transformation triggers only when a threshold value of total plastic strain produced by surface treatment and cyclic loading is exceeded. It seems that this threshold value was not reached for the turned and cyclic loaded sample at a strain rate of 1% whereas it was reached for the sample receiving brushing treatment before cyclic loading. This result can be explained by the significant prior high surface hardening induced by the wire brush hammering operation compared to surface hardening induced by turning as illustrated in Fig. 7. The threshold value of plastic cyclic strain to induce martensite phase was reported by other investigators [21–24]. Krupp et al. reported a value of around 3% for AISI 301 and 304 [23] whereas the same value was reported by Bayerlein et al. for AISI 304L stainless steel [22]. Haušild reported a value of plastic strain lower than 2% for the transformation to occur during tensile tests of AISI 301 [24]. The amount of $\acute{\alpha}$-martensite which depends on the rate of plastic deformation induces a compressive residual stress reaching values on the surface of −506 MPa and −309 MPa in the loading and transverse directions respectively at a strain rate of 1% for the wire brush hammered surface as shown in Table 8.

It was found in this study, that under strain controlled fatigue, the resulting effects of the induced martensite during fatigue loading on wire brush hammered samples produces an excessive strengthening compared to the turned case as seen in Fig. 9a and b. Based on this observation, the negative effect of the induced phase would limit the use of the mechanical brushing as a method to improve fatigue lifetime. Therefore, it was found that this hardening can be beneficial only for strain rates lower than 0.5% in order to avoid the formation of the matensitic phase.

The role of martensite induced by cyclic deformation at strain rate $\Delta\varepsilon_t/2$ = 1% can be explained by two competing effects:

- A beneficial effect in which compressive residual stress is induced and is associated with the volume change [21,23,24].
- A negative effect associated with the excessive strengthening of the material as a result of interaction between dislocations and repeated germination of the induced phase [23,25].

Moreover, the influence of the martensite induced by plastic deformation on crack initiation and propagation resistance of brushed surfaces has been studied by SEM observations. Fig. 11 illustrates the relatively low levels of transformed $\acute{\alpha}$-martensite in AISI 304 steel but these quantities do not improve significantly the low cycle fatigue resistance as observed in other stable grades. In contrast, these quantities seem to degrade the fatigue resistance as observed in Table 7.

4.2. Fatigue life improvement resulting from intermitted brushing operation

It is shown in this study that intermitted brushing that could be executed on site on AISI stainless steel components can indeed improve the residual fatigue life of the component. However, this

Table 9
Cyclic loading residual stresses for turned and brushed surfaces for different imposed strain rates.

Imposed strain rate $\Delta\varepsilon_t/2$ (%)	Surface preparation mode			
	Turned surface residual stress		Brushed surface residual stress	
	Loading direction	Transverse direction	Loading direction	Transverse direction
Unloaded	476	339	−750 ± 20	−622 ± 20
0.1	N.R.	N.R.	N.R.	N.R.
0.2	N.R.	N.R.	N.R.	N.R.
0.3	−346 ± 50	450 ± 58	−639 ± 62	−600 ± 71
0.5	−105 ± 26	212 ± 49	−494 ± 92	−443 ± 90
0.7	−35 ± 35	106 ± 34	−286 ± 103	−306 ± 54
1	−449 ± 63	407 ± 109	−506 ± 68	−309 ± 85

N.R.: no significant relaxation observed.

improvement can be realized for strain rates lower than 0.5 and when performed early in the service lifetime characterized by N_i/N_r lower than 0.5. As it is reported in Table 8, at a $N_i/N_r = 0.25$, the improvement rate of the residual lifetime is reduced from 53% at a strain rate $\Delta\varepsilon_t/2 = 0.2\%$ to 24% at a strain rate $\Delta\varepsilon_t/2 = 0.5\%$. This improvement is, as discussed previously, the result of enhancement of surface texture, surface cold work hardening and compressive residual stress induced by the brushing operation. In addition, it is also reported that this improvement is strain rate dependent.

5. Conclusions

Based on the investigation of the effects of the brushing operation as a method to improve service fatigue life of components in AISI 304 stainless steel, the following conclusions can be made:

- Wire brush hammering operation did not alter significantly the surface topography in terms of roughness but it reduced significantly the surface grooves produced during turning operation and increased significantly the surface hardness from around 180 to 500 Hv. In addition, wire brush hammering produced short fatigue cracks of the order of 50 μm compared to those generated on the turned surfaces that were over 200 μm in length.
- As a result of wire brush hammering operation, residual stress field shifted from tensile to compressive resulting in a significant increase in the crack initiation and propagation resistance. Hence, an increase of fatigue lifetime by over 300% has been achieved for low strain rate of $\Delta\varepsilon_t/2 = 0.2\%$. As the strain rate is increased, the beneficial effects of brushing are reduced due to the compressive residual stress relaxation.
- At high strain rate of $\Delta\varepsilon_t/2 = 1\%$, strain induced phase martensite transformation occurred and reduced or annihilated the beneficial effects of the brushing operation by producing excessive strengthening of the material due to the interactions between the deformation mechanism and the induced phase.
- The intermitted brushing was found to be beneficial if performed in the early stage of the component service lifetime ($N_i/N_r \leqslant 0.3$) and for strain rates lower than 0.5%.

References

[1] Sano Y, Obata M, Kubo T, Mukai N, Yoda M, Masaki K, et al. Retardation of crack initiation and growth in austenitic stainless steels by laser peening without protective coating. Mater Sci Eng A 2006;417:334–40.

[2] Nikitin I, Scholtes B, Maier HJ, Altenberger I. High temperature fatigue behavior and residual stress stability of laser-shock peened and deep rolled austenitic steel AISI 304. Scr Mater 2004;50:1345–50.

[3] Fathallah R, Laamouri A, Sidhom H, Braham C. High cycle fatigue behavior prediction of shot-peened parts. Int J Fatigue 2004;26:1053–67.

[4] Mhaede M. Influence of surface treatments on surface layer properties, fatigue and corrosion fatigue performance of AA7075 T7. Mater Des 2012;41:61–6.

[5] Sadeler R, Akbulut M, Atasoy S. Influence of mechanical (ball burnishing) surface treatment on fatigue behaviour of AISI 1045 steel. Kovove Materialy 2013;51(1):31–5.

[6] Ben Fredj N, Ben Nasr M, Ben Rhouma A, Braham C, Sidhom H. Fatigue life improvements of the AISI 304 stainless steel ground surfaces by wire brushing. J Mater Eng Perform 2004;13(5):564–74.

[7] Sidhom N, Sidhom H, Braham C, Lédion J. Effects of brushing and shot-peening residual stresses on the fatigue resistance of machined metal surfaces: experimental and predicting approaches. Mater Sci Forum 2011;681:290–5.

[8] Brinksmeier E, Garbrecht M, Meyer D. Cold surface hardening. CIRP Annals – Manufacturing Technology 2008; 57: 541-4.

[9] Nikitin I, Besel M. Correlation between residual stress and plastic strain amplitude during low cycle fatigue of mechanically surface treated austenitic stainless steel AISI 304 and ferritic–perlitic steel SAE 1045. Mater Sci Eng A 2008;491:297–303.

[10] Ben Rhouma A, Braham C, Fitzpatrick ME, Lédion J et Sidhom H. Effects of surface preparation on pitting resistance, residual stress and stress corrosion cracking in austenitic stainless steels. J Mater Eng Perform 2001;10:507–14.

[11] Smaga M, Walther F, Eifler D. Deformation-induced martensitic transformation in metastable austenitic steels. Mater Sci Eng A 2008;483–484:394–7.

[12] Mertinger V, Nagy E, Tranta F, Solyom J. Strain-induced martensitic transformation in textured austenitic stainless steels. Mater Sci Eng A 2008;481–482:718–22.

[13] Mei Z, Morris Jr JW. Influence of deformation-induced martensite on fatigue crack propagation in 304-type steels. Metall Trans A 1990;21A:3137–52.

[14] Topic M, Tait RB, Allen C. The fatigue behavior of metastable (AISI-304) austenitic stainless steel wires. Int J fatigue 2007;29:656–65.

[15] NF EN 15305 Avril 2009. Essais non-destructifs: méthode d'essai pour l'analyse des contraintes résiduelles par diffraction des rayons X. AFNOR. 2009.

[16] Sidhom N, Braham C, Lieurade HP. Fatigue life evaluation of shot peened al-alloys 5083 H11 T-welded joints by experimental and numerical approaches. Welding in the World 2007;51(1–2):50–7.

[17] Sidhom N, Laamouri A, Fathallah R, Braham C, Lieurade HP. Fatigue strength improvement of 5083 H11 Al-alloy T-welded joints by shot peening: experimental characterization and predictive approach. Int J Fatigue 2005;27(7):729–45.

[18] De Los Rios ER, Walley A, Milan MT, Hammersley G. Fatigue crack initiation and propagation on shot-peened surfaces in A316 stainless steel. Int J Fatigue 1995;17(7):493–9.

[19] Fathallah R, Sidhom H, Braham C, Castex L. Effect of surface properties on high cycle fatigue behaviour of shot peened ductile steel. Mater Sci Technol 2003;19(8,1):1050–6.

[20] Ghanem F. Ben Fredj N, Sidhom H, Braham C. Effects of finishing processes on the fatigue life improvements of electro-machined surfaces of tool steel. Int J Adv Manuf Technol 2011;52(5–8):583–95.

[21] Krupp U, Christ H-J, Lezuo P, Maier HJ, Teteruk RG. Influence of carbon concentration on martensitic transformation in metastable austenitic steels under cyclic loading conditions. Mater Sci Eng A 2001;319–321:527–30.

[22] Bayerlein M, Christ H-J, Mughrabi H. Plasticity-induced martensitic transformation during cyclic deformation of AISI 304L stainless steel. Lett Mater Sci Eng A 1989;114:L11–6.

[23] Krupp U, West C, Christ H-J. Deformation-induced martensitic formation during cyclic deformation of metastable austenitic steel: Influence of temperature and carbon content. Mater Sci Eng A 2008;481–482:713–7.

[24] Haušild P, Davydov V, Drahokoupil J, Landa M, Pilvin P. Characterization of strain-induced martensitic transformation in a metastable austenitic stainless steel. Mater Des 2010;31:1821–7.

[25] Ye D, Matsuoka S, Nagashima N, Suzuki N. The low-cycle fatigue and final fracture behavior of an austenitic stainless steel. Mater Sci Eng A 2006;415:104–17.